Assessment of Olefin-Based IUD Tail Strings

David Roylance

Department of Materials Science and Engineering, Massachusetts Institute of Technology, Cambridge, Massachusetts

The "tail string" that extends from a contraceptive intrauterine device (IUD) into the vagina is an illustrative case in materials engineering design. The strings must satisfy certain criteria for strength and other properties in order to fulfill the function of providing a means of insuring that the IUD has not been ejected, and eventually of helping remove the IUD. This must be done without contributing to an additional risk of unwanted medical side effects beyond those that may be inherent in any such device. Oriented monofilament olefins appear to satisfy these criteria, and have been used successfully in several IUD designs. This article describes a study of two such monofilaments taken from new IUDs, showing how the material's processing, structure, and properties lead to effective performance as tail strings. Several types of used IUDs were also studied, to insure that nothing occurred during use that would alter the conclusions drawn from the study of new strings. © 1993 John Wiley & Sons, Inc.

INTRODUCTION

Intrauterine contraceptive devices often employ a filamentary tail string (see Fig. 1) that is used both to assist in the eventual removal of the device and as an indicator that the device has not been expelled prematurely.[1] The string must satisfy a number of physical criteria to assure proper function and safety. We have examined two types of olefinic tail strings from a materials engineering perspective to assess the extent to which they satisfy these criteria. Our methods and conclusions differ substantially from those of a recent paper by Warner et al.[2] These authors are critical of the choice of polypropylene as an IUD string, based largely on their interpretations of optical and electron micrographs.

We can list several criteria that should be met in a successful IUD tail string design:

- The string must have sufficient tensile strength to avoid breakage during IUD removal, while still being small in diameter to provide flexibility.
- The string material should be biologically inert, that is, should not undergo chemical or physical change during use that would increase the incidence of a side effect or result in a degree of degradation that would impair the string's function.
- Given the controversy over the Dalkon Shield multi-filamentary tail string, it would appear prudent to use a hydrophobic monofilament, so that water absorption (and conceivably, capillary transport) is avoided.
- The string must be capable of attachment to the body of the IUD by a method that does not result in a loss of tensile strength.
- The string must be capable of being sterilized, by either chemical or thermal means.
- The string should be capable of being colored, to aid in distinguishing it from surrounding tissue.
- The string material should preferably be widely available, and capable of being processed to create a string of consistently high quality.
- The string material should have a proven history of safe and effective use in biomedical applications.

As will be demonstrated, the design criteria for tail strings are met by olefin (specifically polyethylene and polypropylene) polymers that have been extruded as monofilaments and then stretched ("drawn") to produce a fiber approximately 0.01″ in diameter with a preferred molecular orientation along the fiber axis. The chemistry and microstructure of these materials, and how they result in a profile of engineering properties appropriate to an IUD tail string are described.
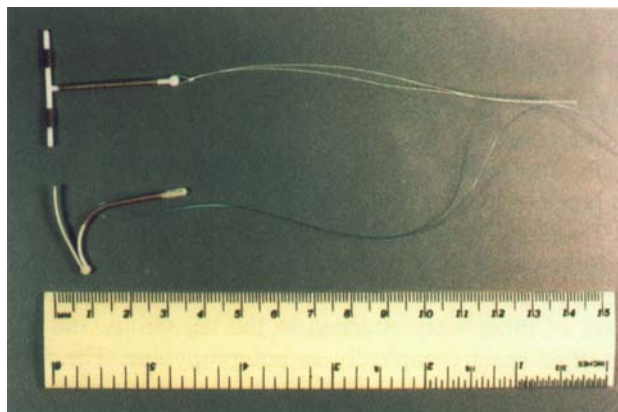

Figure 1. GynoPharma ParaGard (upper) and Searle Cu-7 (lower) intrauterine devices.

EXPERIMENTAL STUDIES
OF UNUSED IUD STRINGS

Two types of unused commercial IUDs, both using olefin tail strings, were obtained: the "ParaGard," distributed by GynoPharma, Inc., and the "Cu-7," distributed by Searle Pharmaceuticals Inc. The devices were received in their original unopened sterile packages, and handled only with gloves or plastic tweezers when microscopy or surface-energy tests were to be done. As seen in Figure 1, the Cu-7 device has a single tail string, approximately 11″ long, which is attached to the body of the IUD by melt bonding. In contrast, the tail string of the ParaGard device is attached by knotting, giving two tails each approximately 4.2″ long.

Material Identification

The chemical identity of the tail string materials was determined by infrared (IR) spectroscopy, which identified the ParaGard and Cu-7 tail strings as polyethylene and isotactic polypropylene, respectively. This identification was based on visual comparison of the IR spectra with published standard spectra, and was not capable of determining the presence of small concentrations of additives such as colorants or antioxidants. The identification of the Cu-7 string as polypropylene is consistent with manufacturer's records[3] that specify Hercules ProFax 6523 resin, a general-purpose polypropylene resin formulated specifically for manufacture of fiber.

Fibrils were observed clinging to the tail strings of some IUDs upon removal from their packages. Warner et al.[2] claim fibrillation may be a health hazard, speculating that the increased surface area attributable to fibrillation might permit additional bacterial colonization of the string. Although this contention is debatable, it was considered important to determine whether the observed fibrils were part of the string itself or simply airborne fibrous debris attracted to the string by the static electrical charge that develops naturally when the string is handled or even simply slid out of its container. To this end, a number of "micro-FTIR" analyses were performed in which an optical microscope is used to isolate and mask off the fibril in question, and the IR beam then directed only to that material.

One ParaGard and one Cu-7 were examined by micro-FTIR. The technique was able to differentiate between the types of polyethylene used in the ParaGard string and its Tyvek package backing, and also identified the five fibrils found on the ParaGard as four cotton and one nylon strands. Four fibrils were found on the Cu-7 examined. Three of these were attached to the tail string, and were identified spectroscopically as polypropylene. The fourth fibril was cotton.

As will also be shown below by electron microscopy, a minor degree of true fibrillation is occasionally present on the olefin string surfaces. But micro-FTIR shows that surface debris can easily lead to an incorrect conclusion regarding the extent of fibrillation, if determined by microscopy alone. This is especially true for used tail strings. All objects, regardless of material composition, rapidly acquire a "biofilm"[4] within the body that can obscure the material's surface. Additionally, cotton or other fibers from tampons or laboratory swabs might be expected to adhere to the tail string; Warner et al.[2] show micrographs that may well be dominated by such debris. Those authors do not report having confirmed the identity of what are represented to be frays of polypropylene by micro-FTIR or other definitive techniques.

Molecular Weight

The molecular weight distributions for both polyethylene and polypropylene strings were determined by high-temperature gel permeation chromatography (GPC). The specimens were dissolved in trichlorobenzene, and separated by "JordiGel" columns operating at 145 °C. The polymer was protected from degradative oxidation during chromatography by N-phenyl-2–napthylamine. The raw data were calibrated initially using polystyrene standards, and these results then further calibrated by reference to specimens of polyethylene and polypropylene whose molecular weight had been determined by light scattering.

Typical reduced chromatograms are shown in Figure 2, which reveals the polyethylene material to be generally higher in molecular weight than the polypropylene. The molecular weights are as expected for Ziegler-polymerized olefins, although the weight-average molecular weight for the polypropylene is lower than the approximately 300,000 gm/mol cited by Ahmed[5] for 65XX-series ProFax resins. The polypropylene molecular weight may have been reduced somewhat by the spinning process because this material is prone to thermally induced oxidation and chain scission at the temperatures associated with melt processing.
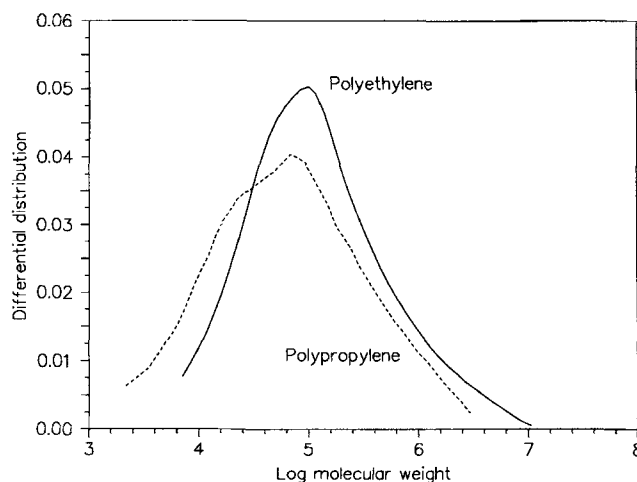

Figure 2. Molecular weight distributions of IUD tail string materials as determined by high temperature gel permeation chromatography.

The reproducibility of the GPC analysis was assessed by subjecting the polypropylene string to three independent replications, each using a new IUD specimen. The molecular weight averages obtained in these three tests are shown in the table below, which also includes the averages of the single polyethylene string analyzed. Each set of values is the average of two GPC chromatograms, obtained from two injections of the same batch of dissolved polymer.

Material	$\bar{M}_n$	$\bar{M}_w$	D
Polypropylene	22,300	181,000	8.11
Polypropylene	24,700	206,000	8.38
Polypropylene	25,900	197,000	7.61
Polyethylene	48,300	359,000	7.43

Here $\bar{M}_n$ and $\bar{M}_w$ are the number and weight average molecular weights, respectively, and $D = \bar{M}_w/\bar{M}_n$ is the dispersivity.

Thermal Properties

Figure 3 shows thermograms obtained by differential scanning calorimetry (DSC) for the polypropylene and polyethylene string materials. The specimens were tested in clinched aluminum pans, with an argon atmosphere. The peak observed in each thermogram represents melting of the crystalline phase within the material, with the area under the peak being the crystalline heat of melting. The crystallites in polyethylene are more tightly packed than in polypropylene due to the simpler polyethylene molecule. This tighter crystalline bonding in polyethylene, coupled with its higher crystalline fraction, leads to a higher overall heat of fusion. However, the lesser chain flexibility of the more complex polypropylene molecule produces a higher melting temperature in polypropylene.

Note in Figure 3 that the polypropylene melting that peaks at 167 °C begins with a low-temperature "tail" beginning at approximately 140 °C. This behavior, which is absent in the polyethylene material, may help explain why polypropylene is amenable to heat bonding to the IUD body, but polyethylene is not. After some practice with a heat gun, an operator can induce softening but not complete liquification in the polypropylene by heating into the tail region of the thermogram; polyethylene with its much more abrupt melting cannot be partially melted in this manner.

Five DSC replications were performed on each of the two materials, yielding the following averages for the melting temperature T_m and heat of crystalline melting ΔH (the values in parentheses are the coefficients of variability, defined as the ratio of the standard deviation to the mean).

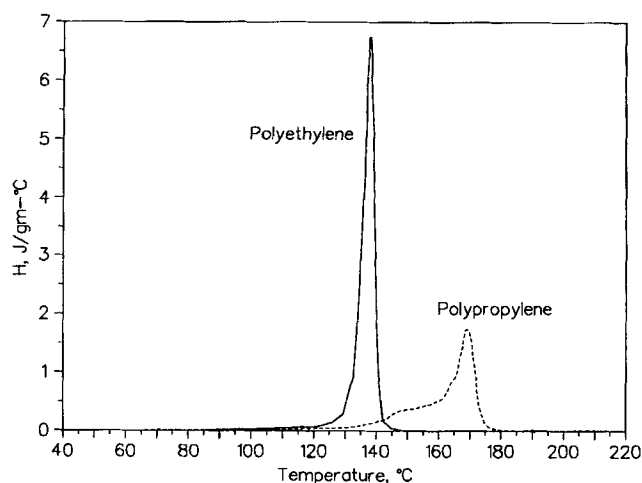|	Polyethylene	Polypropylene
$T_m(°C)$	133.22 (0.68%)	162.81 (0.36%)
$\Delta H(J/g)$	244.4 (2.32%)	99.89 (2.00%)

Figure 3. DSC thermograms for tail string materials.

The measured heats of melting were used to determine the percent crystallinity in the two materials. Using a value of 170 J/g for the polypropylene crystal heat of melting[6] and neglecting the presence of colorants and other additives, the measured average heat of fusion of 99.89 J/g for polypropylene corresponds to a crystallinity of 59% and a density of $\rho = 0.902$. The values for the polyethylene are very close to those reported[7] for Marlex 50, a highly linear polyethylene with 91% crystallinity and a density of $\rho = 0.965$; this material has $T_m = 135$ °C and $\Delta H = 245.3$ J/g.

Dynamic mechanical analysis (DMA) was used to probe the dependence of the strings' mechanical properties on temperature. Figure 4 displays the storage modulus for both polyethylene and polypropylene strings as measured with a RheoVibron Viscoelastometer, over a temperature range from near liquid nitrogen temperature up to specimen melting. The scans for the polyethylene and polypropylene strings are similar, showing no important transitions over the range of temperatures expected in clinical practice. A small relaxation corresponding to the glass transition of the amorphous segment in the polypropylene is seen in the range of approximately 0–20 °C. The higher melting temperature of the polypropylene is evident in these data as well.

Optical Microscopy

The tail strings were examined by optical microscopy for general appearance and to determine their diameters. The polyethylene strings were white in appearance, perhaps due to the use of a titanium dioxide or similar pigment. The polypropylene was blue in appearance, being colored with an organic pigment on an aluminum oxide particulate carrier.[3]

The strings were examined in their pristine state, specifically without etching their surfaces. In their optical microscopic observations, Warner et al.[2] made extensive use

of a chromic acid etching treatment proposed by Armond and Atkinson[8] for enhancing the image of spherulitic polypropylene by removing the noncrystalline molecular structure. Features observed after such a treatment have been artificially created or exaggerated by the investigator, and may lead to incorrect inferences if used to assess the quality of the material.

Both polyethylene and polypropylene strings were examined with polarized light microscopy, using objectives ranging from 40 to 100×. The polypropylene strings are translucent, enabling observation of interior features within the string. No internal features were visible within the polyethylene strings, although a number of what appeared to be kink bands were visible at approximately ±45° from the fiber axis. By contrast, the colorant particles were easily seen at various depths within the polypropylene string. Surrounding each of these particles were elongated structures known to fiber processors as "breakout" voids, formed as the polymer is drawn away from the rigid particle. These regions were not measured or counted in our work, although Warner et al.[2] state that 64% of the features are less than 10 μm in length, with some as long as 250 μm. Figure 5 shows such a region, in this case containing multiple colorant particles. These features were not observed to interconnect. Based on optical microscopy alone it is difficult to state whether these voids communicate with the surface. This issue will be addressed in the discussion of electron microscopy.

The void content associated with particulate breakout or other drawing-induced effects can be computed by comparing the actual measured densities of the fibers with the densities known for the crystalline and amorphous phases, along with the percent crystallinity determined from calorimetric measurements as described earlier. Actual densities were measured by noting the equilibrium positions of 1/4″-long specimens in an isopropyl alcohol–diethylene glycol linear density gradient column. The specific gravities of the polyethylene and polypropylene
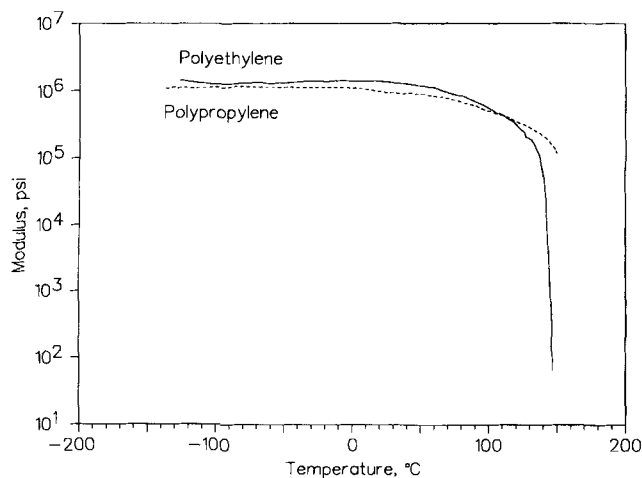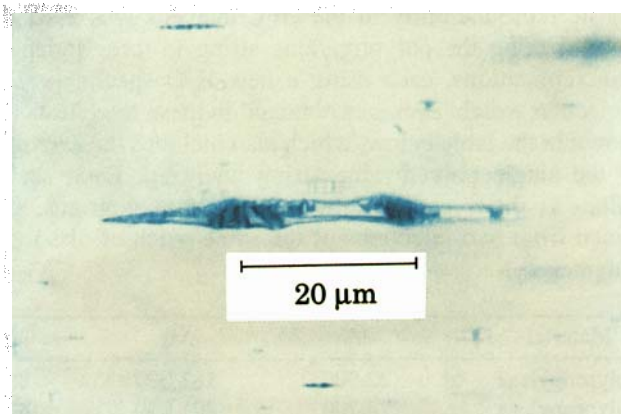

Figure 5. Optical micrograph showing colorant particles and associated breakout region in the interior of polypropylene fiber.
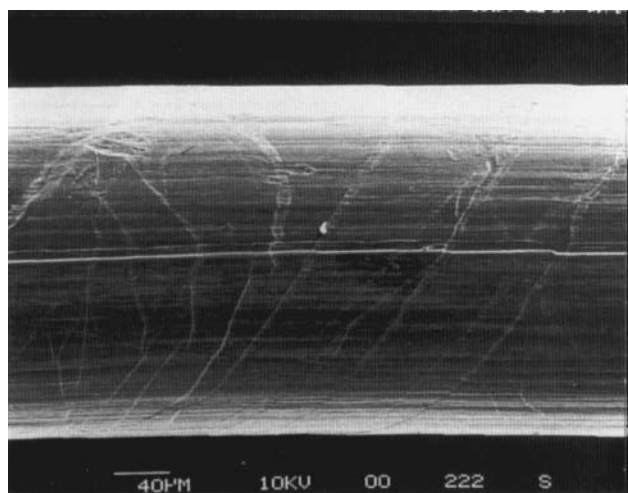
strings were measured to be 0.950 and 0.856, respectively, as compared with the calorimetric values of 0.965 and 0.902. The volumetric void content is thus 1.55% for the polyethylene string and 5.10% for the polypropylene.

Statistical measures of the string diameters were obtained by using a calibrated microscope reticule to measure the width of the fiber when viewed from the side. The widths were measured every 10 degrees as the fiber was rotated around its long axis, and at 1″ intervals along its length. The diameters of the polypropylene varied from a minimum of 0.00876″ to a maximum of 0.0122″, but its average diameter of 0.0107″ was uniform along the length (1.4% coefficient of variability). The polyethylene string is nearly circular, with an average diameter of 0.0103″ and a coefficient of variability with respect to axial rotation of 2.25%.
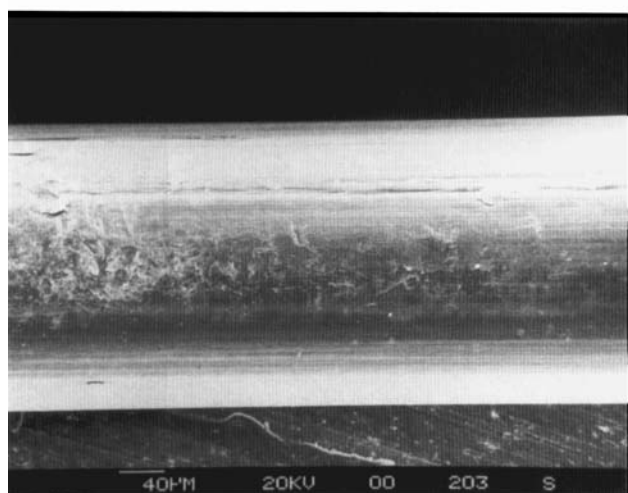
Scanning Electron Microscopy

Scanning electron micrographs were obtained from both polyethylene and polypropylene tail strings in four configurations: as received, with a tight single knot, split to show internal failure surfaces, and cut both longitudinally and transversely with a fresh razor blade.

As seen in Figure 6, the polyethylene and polypropylene tail strings appear similar on microscopic examination, each showing evidence of longitudinal scratches (presumably from microscopic irregularities in the spinneret) and occasional delaminations. The secondary electrons observed in this SEM mode come from only the top few nanometers at the surface, so that unlike optical microscopy there is no ambiguity as to whether observed features are at the surface or within the material. In scanning several specimens along their entire length, no voids that could be associated with particulate breakout were observed at the surface of either the polyethylene or polypropylene strings. Evidently the flow field during spinning acts to submerge the colorant particles, so that the breakout regions are confined to the interior of the string.
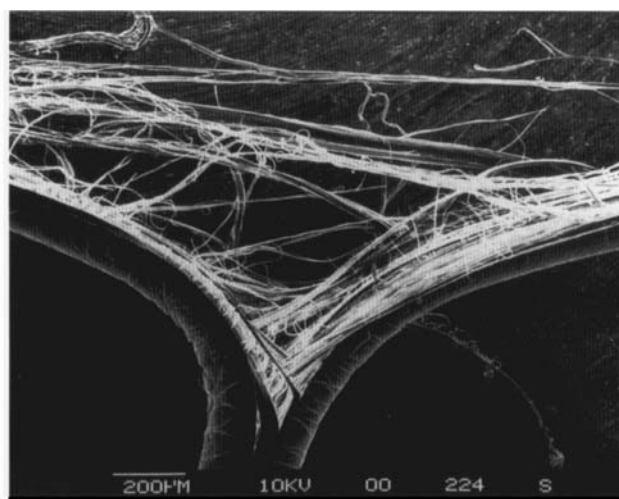

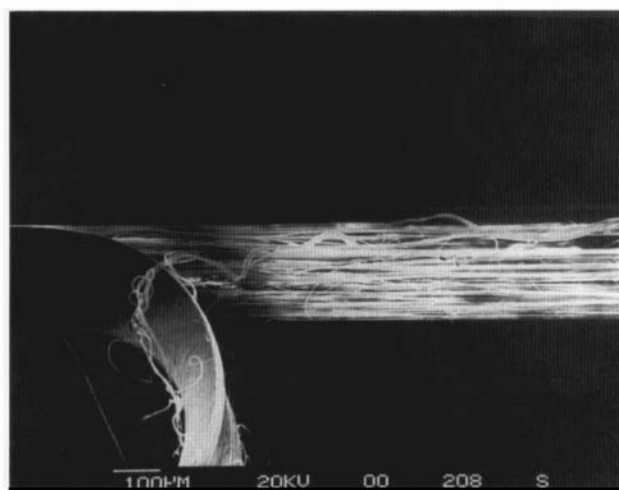**Figure 4.** Dynamic mechanical response of polypropylene and polyethylene materials, tested at 11 Hz cyclic frequency.

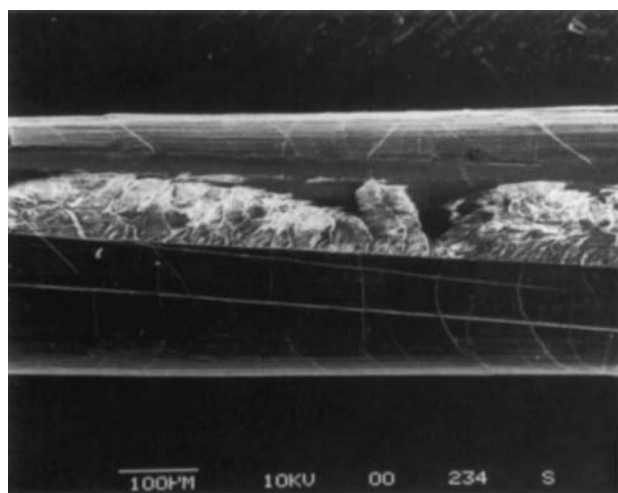**Figure 6.** Scanning electron micrographs of polyethylene (a, nominal 220× magnification) and polypropylene (b, 170×).

Figure 7. Scanning electron micrographs of manually split polyethylene (a, 60×) and polypropylene (b, 60×).

When split longitudinally by starting a separation with a scapel and then advancing the split manually, fracture surfaces propagate along the directions of molecular orientation to create a series of visible fibrils; Figure 7 shows micrographs of such a split in the two strings. The two strings appear to exhibit similar behavior on manual splitting, but with noticeably more fibrillation in the polyethylene. The micrographs did not show evidence of discrete impurities or additives, such as the colorant particles, or such features as breakout voids that might have been caused by them. It does not appear that the propagating fracture surface seeks out or is assisted by breakout regions.

When sliced with a razor blade, the cut surfaces do not exhibit significant fibrillation. Figure 8 shows room-temperature sections of polyethylene and polypropylene strings, respectively. This serves as a reminder that the interior features observed after cutting or tearing are influenced strongly by the manner in which the fracture surface was created, so that caution is needed in using such micrographs to characterize the material's microstructure.

Although fibrillation can be induced in the drawn olefin strings by forcing a fracture plane through the material as shown above, the strings are able to remain relatively free of fibrillation under even rather severe mechanical abuse. This can be demonstrated qualitatively by tying a tight knot in the string (Fig. 9). The knotting develops substantial compressive or tensile strains on the concave and convex surfaces of the knot, respectively. Figure 9 shows that the stain-induced damage consists of only minor fibrillation on the tensile surfaces and compressive buckling on the concave surfaces. More fibrillation is observed in the polypropylene string than in the polyethylene, although it is not possible to state that the fibrils present in Figure 9(b) were created by the knotting rather than being present previously. Although it
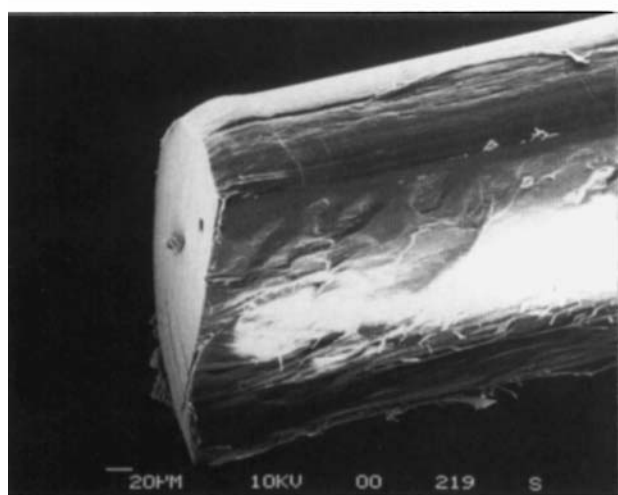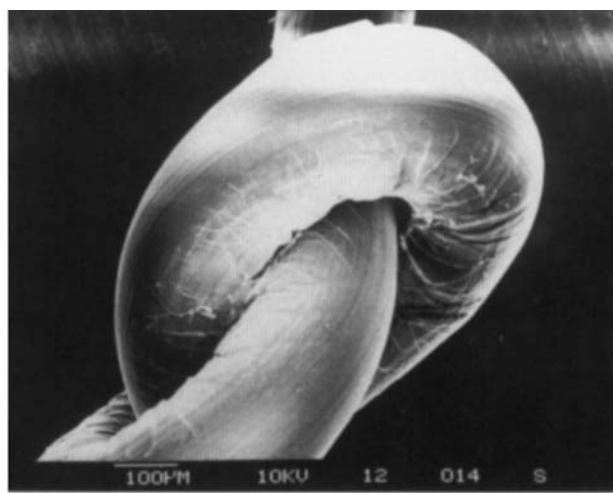
Figure 8. Scanning electron micrographs of polyethylene (a) and polypropylene (b) cut with a razor blade at room temperature.

Figure 9. Scanning electron micrographs of knotted polyethylene (a, 90×) and polypropylene (b, 59×) strings.
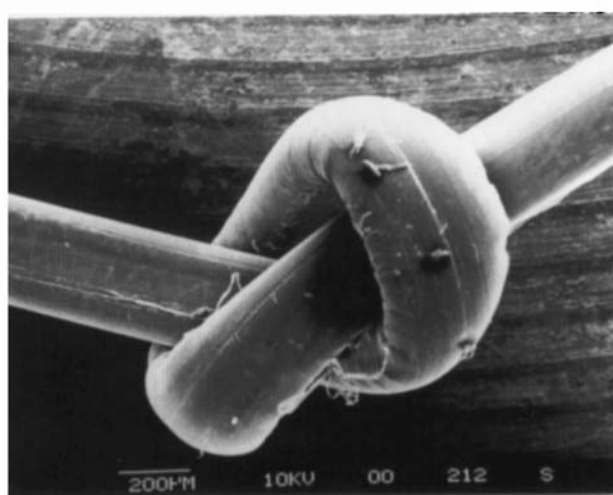
is possible that some IUD strings would develop enough fibrillation in processing or handling to be rejected on appearance grounds, the minor fibrillation observed in our studies would not be sufficient to reduce the mechanical strength of the string. Neither do they seem numerous enough to produce an appreciable increase in the string's surface area.

Surface Energetics and Solubility

Polyolefins such as polyethylene and polypropylene are expected to be low surface energy materials consisting primarily of carbon and hydrogen, for which solid–liquid interactions should be dominated by low-energy dispersive mechanisms. Surface energetics of the polyethylene and polypropylene strings were determined by the Wilhemy technique[9] in which an electrobalance is used to measure the change in apparent mass caused by wetting forces

as the string is lowered into and raised from a liquid of known surface energy.

The dispersive component of filament surface energy γ_s^d was measured by using a nonpolar material (methylene iodide) as the probe liquid; the results gave values of 32.2 and 24.1 mN/m for polyethylene and polypropylene, respectively. Repeating the experiment with polar probe liquids (formamide, ethylene glycol, water) showed the tail strings had negligible acid–base surface character, as might have been introduced by surface oxidation.

Water does not wet olefin surfaces because water has a high surface tension of $\gamma_L = 72.8$ mN/m (21.8 mN/m dispersive component, 51 mN/m polar component) and its molecules prefer proximity to themselves rather than spreading on the low-energy olefin surface. One measure of this mutual repulsion is the contact angle θ, which can be computed from the work of adhesion W_A as

$$W_A = \gamma_L(1 + \cos\theta).$$

The work of adhesion between the tail string materials and water was measured to be 57.1 and 52.7 mN/m for polyethylene and polypropylene, respectively. The coefficient of variation of this measurement was 3.5% for the polyethylene strings (five specimens) and 9.7% for the polypropylene (seven specimens). The work of adhesion for both string materials was measured to be dominantly dispersive in nature, with a near-negligible polar component. The resulting contact angle is 102° for polyethylene and 106° for polypropylene, which indicates quantitatively that water will bead up rather than wet or climb a polyolefin surface.

The lack of affinity between olefins and water can be expected to lead to a very low uptake of moisture in humid environments. To measure this directly, fiber weights were determined in air before and after 3 days' total immersion in distilled water. As seen in the table below showing measurements from four specimens of each material, both polyethylene and polypropylene strings exhibit negligible water uptake.

Specimen	% Weight Change
Polyethylene	−0.02
	−0.10
	+0.08
	+0.13
Polypropylene	−0.06
	−0.01
	+0.44
	+0.52

The above tests directly address the question of fluids being carried up the tail string by capillary action: these strings have a low surface area due to their monofilament construction, effective capillary channels are not present, and the olefin strings are inherently water-repelling.

The data reduction in Wilhemy testing requires that the fiber perimeter length be known, and this was measured by weighing each fiber specimen in and out of a liquid capable of wetting the fiber completely (hexane). The effective diameters calculated from these perimeters were 0.00926″ for the polyethylene strings (21 string specimens, coefficient of variability 1.5%) and 0.0114″ for the polypropylene strings (22 specimens, variability 2.3%). These diameters are very near those obtained by optical microscopy (10% smaller in the case of the polyethylene fibers, 6.5% larger for the polypropylene). In addition to providing a check on the fiber size, this wetting result implies that the fibers are free of extensive fibrillation or interconnected voids that provide a pathway for liquid to infiltrate the fiber interior. Both of these would increase the wetting surface area, and yield much increased values of effective fiber diameter.

Molecular Orientation

The mechanical properties of the tail strings are influenced strongly by molecular orientation imparted to the material during processing. Several measurable properties of polymers are related to the orientation of the molecular structure, and this provides an indirect means of determining this important parameter. One such property is the "sonic" modulus, which is related to the wavespeed of acoustic pulses in the material by

$$E = \rho c^2$$

where E is the modulus, ρ is the density, and c is the wavespeed. The mean deviation of the molecular chains from the fiber axis as given by the mean square cosine of the inclination angle $\langle \cos^2 \phi \rangle$ can be found from the ratio of the wavespeeds in the unoriented and oriented polymer[10]:

$$\langle \cos^2 \phi \rangle = 1 - \frac{2}{3} \frac{c_u^2}{c^2} = 1 - \frac{2}{3} \frac{E_u}{E}$$

where the u subscript refers to values for unoriented polymer. The value of E_u for polypropylene is 407 kpsi,[11] and the corresponding value for polyethylene (Marlex 50) is 440 kpsi.[12] Orientation is often stated in terms of the "Hermans orientation function," which is related to the mean square cosine as

$$f = \frac{3\langle \cos^2 \phi \rangle - 1}{2}.$$

This parameter is a useful measure of overall orientation, being equal to 1.0 for perfect molecular alignment along the fiber axis, 0.0 for random molecular orientation, and −0.5 for perfect orientation in the direction perpendicular to the fiber (transverse orientation).

The wavespeeds of the polyethylene and polypropylene strings were measured using a Morgan PPM-5 Pulse Propagation Meter,[13] and these data were used to calculate the orientation parameters in the following table:

	Polyethylene	Polypropylene
c (km/s)	3.37	3.60 (2.25%)
E(Mpsi)	1.59	1.89 (4.43%)
f	0.723	0.780 (1.30%)

The coefficients of variation given in parentheses for the polypropylene strings were obtained from independent measurements of 10 specimens drawn from the same lot used for the strength tests in this study, which indicates small variability within a given lot. In the case of the polypropylene fiber, it was possible to procure additional specimens drawn randomly from lots representing the entire Cu-7 production history. This permitted the lot-to-lot variability to be assessed for that fiber; sonic modulus

measurements from 12 additional fibers selected as described produced the same mean ($\bar{f} = 0.78$), with only a slightly larger variability (3.54%). This lot-to-lot sampling was not possible for the polyethylene strings, so statistics are not reported for that material.

The crystalline orientations of the strings were measured by wide-angle X-ray diffraction, specifically by measuring the intensity of diffraction $I(\phi)$ from appropriate crystal planes as a function of the angle ϕ between the fiber and the plane of the incident and diffracted X-ray beams.[14] The orientation of the molecular chain axis can be determined directly from the (110) planes in polyethylene because those planes are parallel to the chain axis. However, polypropylene has a monoclinic crystal structure that requires data from two independent planes such as (110) and (040) to determine the chain–axis orientation.[15]

The $I(\phi)$ data were used to compute a mean angular deviation of the selected planes from the fiber axis according to

$$\langle \cos^2 \phi_{hkl} \rangle = \frac{\int_0^{\pi/2} I_{hkl}(\phi) \sin \phi \cos^2 \phi \, d\phi}{\int_0^{\pi/2} I_{hkl}(\phi) \sin \phi \, d\phi}.$$

The mean deviation of the molecular chains (which lie along the crystal c-axis) was then computed as

$$\langle \cos^2 \phi_{c,z} \rangle = \begin{cases} 1 - 2\langle \cos^2 \phi_{110,z} \rangle & \text{polyethylene} \\ 1 - 1.099\langle \cos^2 \phi_{110,z} \rangle \\ \quad - 0.901\langle \cos^2 \phi_{040,z} \rangle & \text{polypropylene} \end{cases}$$

Finally, the crystalline orientation function was computed as

$$f_c = \frac{3\langle \cos^2 \phi_{c,z} \rangle - 1}{2} = \begin{cases} 0.704 & \text{polyethylene} \\ 0.701 & \text{polypropylene} \end{cases}.$$

The overall orientation f is the weighted average of the crystalline and amorphous orientations f_c and f_{am} respectively: $f = \beta f_c + (1 - \beta)f_{am}$, where β is the fractional crystallinity. Knowing the crystalline fraction from calorimetry, the overall orientation from the sonic modulus values and the crystalline orientation from X-ray diffraction, the amorphous orientation is calculated as:

$$f_{am} = \frac{f - \beta f_c}{(1 - \beta)} = \begin{cases} 0.92 & \text{polyethylene} \\ 0.89 & \text{polypropylene} \end{cases}.$$

String Strength

A number of load-elongation tests to failure were completed on both polyethylene and polypropylene strings, using a screw-operated Instron tensile testing machine operating at a constant strain rate of 50%/min. The short tail strings on the ParaGard IUD requires that the specimen be gripped by tabs. In order to make the polypropylene tests comparable, the single long string on the Cu-7 was cut into three 4" pieces and each tabbed

similarly to the polyethylenes. Figure 10 compares typical load–strain curves for the two string materials.

Statistics of the measured breaking loads are summarized below: Here n is the number of specimens tested,

	Polyethylene	Polypropylene
n	8	17
$\bar{P}_b$ (lb)	4.60	6.04
s	0.304	0.857
C.V. (%)	6.61	14.2
σ_b (kpsi)	50.2	67.2

$\bar{P}_b$ is the mean breaking load, s is the standard deviation, and C.V. is the coefficient of variation. The values of ultimate tensile stress σ_b were computed by dividing the mean breaking loads by the areas corresponding to the mean fiber diameters determined by optical microscopy.

OBSERVATION OF USED IUD STRINGS

A number of used IUDs of various types were made available for visual and microscopic examination. These devices were collected in Canada during the years 1978–1983, having been retained after removal at the end of their normal (approximately 2 year) usage period. The devices were dried after collection and sterilized with ethylene oxide. In general, examination of the tail strings revealed no signs of degradation during service, although they became partially encrusted with biological debris. Fraying was negligible.

Eleven of these devices were selected at random and retained by this author for more detailed examination and documentation of the tail strings, and Figure 11 shows optical micrographs of two of these. Some apparent fibrillation is seen in the Cu-7 with a black string shown here. However, micro-FTIR identified the large fibril (indicated by arrow) as protein residue, with some others
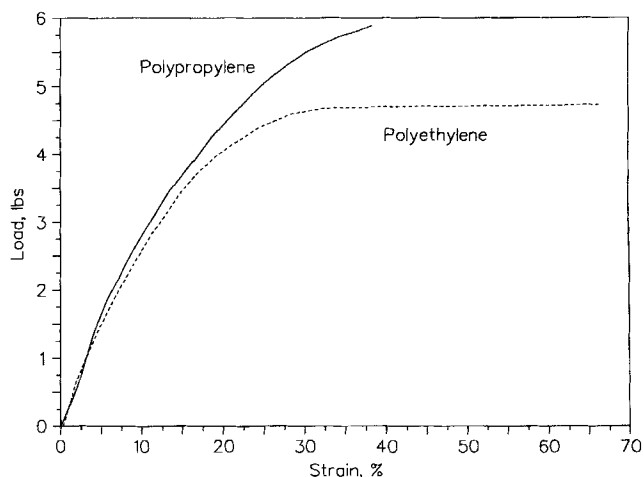

Figure 10. Load–strain response of the polypropylene and polyethylene tail strings.

being polypropylene. As pointed out earlier, it is not true that all fibrillar features observed in microscopy are true frays.

Figure 12 shows four of the optical micrographs obtained during this study, in this case of the region at which the tail string is joined to the IUD body. Figure 13 shows scanning electron micrographs of two of these joints; these show additional detail and also permit a comparison of optical versus electron microscopy. Apart from the general conclusion that the tail strings are not degraded by use within the body, it is evident that the heat bonding method used in the Cu-7 produces a very clean joint, with a lesser tendency to accumulate biological debris.

The overall impression left by the examination of the used strings is that the body environment did not induce any unwanted chemical or physical change in the polymer, and that the properties are likely to have maintained their as-new values during use. This is the expected result, given the well-established chemical and biological stability of olefin materials.

DISCUSSION AND CONCLUSIONS

The total number of strings studied in this work is not large from a clinical standpoint, so it cannot be guaranteed that these findings are representative. In the case of polypropylene strings, however, a wide enough sampling was made to give at least some indication of within-a-lot and lot-to-lot consistency.

Tail string design is a typical application in materials engineering, in that materials properties must be matched against a list of performance criteria, and the properties of selected materials optimized by suitable processing. Some of the tail-string criteria proposed earlier are satisfied by the inherent nature of olefinic polymers, such as the ability to be sterilized by ethylene oxide, and an extensive track record of use in biomedical applications.[16] Other important criteria, especially tensile strength, require that the material be suitably processed to create the necessary oriented microstructure.

Both polyethylene and polypropylene are natural choices for IUD tail strings due to their hydrophobicity, which is a consequence of their aliphatic hydrocarbon constitution. Among the generally available polymers, only polytetrafluoroethylene is more water repellent, and the low tensile strength of that material renders it unsuitable as a tail string. The choice between polyethylene and polypropylene is less clear because these two materials are similar in many respects. As was mentioned earlier, polypropylene is less crystalline than polyethylene, but its inherently stiffer molecular chains compensate for this.

Polypropylene is often selected over polyethylene in applications for which resistance to "environmental stress cracking," or ESC, is important. The ESC phenomenon is related to the tendency of environmental agents such as detergents to plasticize material at the tips of stress-bearing cracks and thus facilitate crack growth. The greater chain stiffness of polypropylene is important in countering this effect. In conservative design, resistance to ESC would probably be considered a beneficial auxiliary factor.

The ability to heat-bond the polypropylene tail string to the IUD body is an important factor that favors that material. In contrast, heat bonding polyethylene can cause an unacceptable weakening of the string, forcing the manufacturer to use a knotted double string. The knot in turn induces strain in the strings as shown earlier by electron microscopy. Further, if minimizing the use of artificial materials in the body is regarded as a prudent design principle, a method of attachment that permits a single strand tail string is preferable.

Such characteristics as hydrophobicity are provided by the inherent chemical nature of the olefin material; achieving the necessary mechanical strength requires that a suitable microstructure be imparted to the monofilament during processing. After leaving the spinneret and cooling from the melt, these materials crystallize by forming platelets termed "lamellae" approximately 100 Å in thickness. At conventional spinning rates, the lamellae grow radially outward from heterogeneous nucleation sites, forming "spherulites" within which the crystal lamellae alternate with uncrystallized amorphous material. Olefin polymer left in this spherulitic state exhibits strengths on the order of 5000 psi, which would require an excessively thick tail string if the needed 4 to 6 lb breaking strength is to be achieved.

The strengths of many semicrystalline polymer filaments can be manipulated over a wide range by tailoring the spinning and drawing operations to align the crystalline and amorphous components of the molecular structure with the fiber axis. As the fiber is drawn to increasingly high stretch ratios after spinning, the spherulitic structure is initially deformed in the stretching direction, and eventually transformed into a "fibrillar" state of much higher strength and stiffness. In this state the original lamellae are broken apart to form a regular sequence of crystalline domains separated by noncrystalline chain segments, some of which act as "tie chains" to permit stress transfer from crystallite to crystallite. This microstructure, which is typical of many synthetic textile fibers, is illustrated in Figure 14.[17,18]

Examination of Figure 14 provides some insight into the tendency of drawn polymer monofilaments to fibrillate occasionally. With most polymer chains aligned along the fiber axis, fewer are available to tie adjacent regions together laterally. When a fiber is split longitudinally, the fracture surface will tend to propagate along the dominant molecular-orientation direction to create a fibrillar fracture surface. However, it is important when considering lateral strength not to take the idealized schematic of Figure 14 too literally. Such diagrams are intended to explain the dramatic increase in strength along the fiber direction that

Figure 11. Optical micrographs of used Cu-7 with black polypropylene string (a) and used "T" with blue polyethylene sting (b), showing debris encrustation.

can be achieved by drawing, and do not portray accurately the many connections that remain available in the lateral direction. It should also be noted in this model that once the spherulite-to-axial transformation has taken place, further drawing would be expected to improve molecular alignment without necessarily diminishing the number
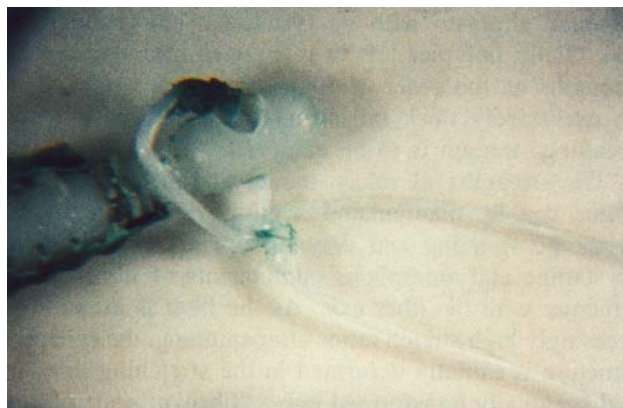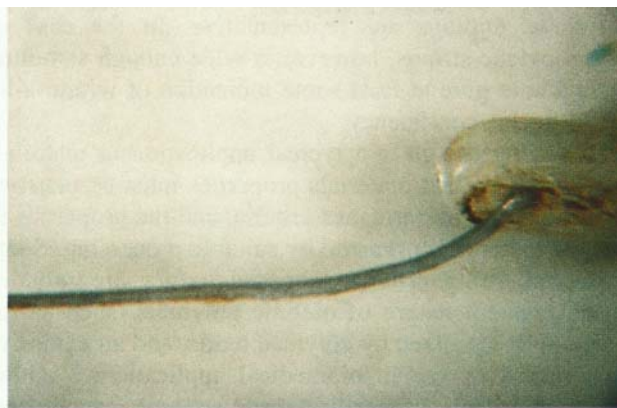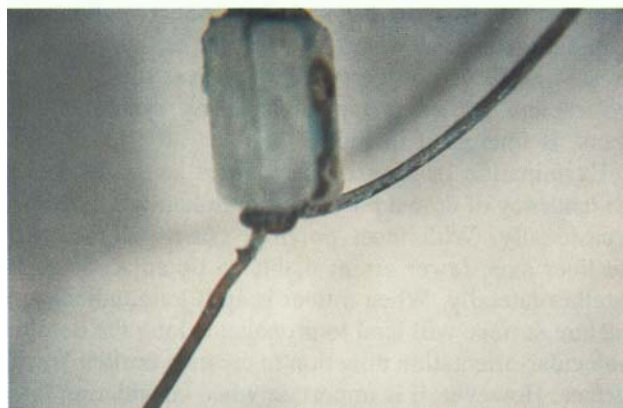

Figure 12. Optical micrographs of string attachment region in various IUDs. (a) "T"; (b) Cu-7; (c) MultiLoad 250; (d) Lippes Loop.
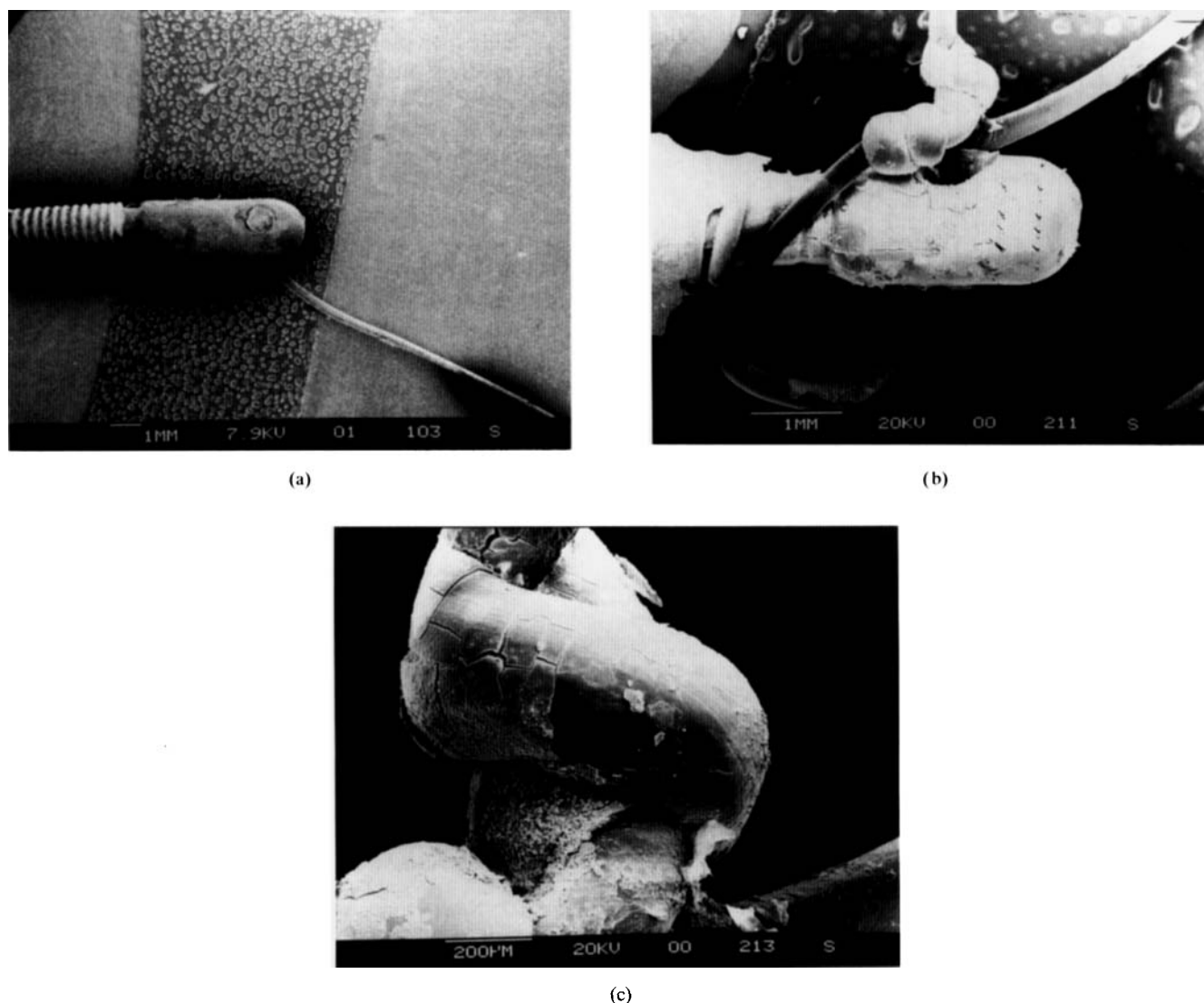
(a)

(b)

(c)

Figure 13. Scanning electron micrographs of attachment region: (a) Cu-7 at 4×; (b) "T" at 17×; (c) Cu-T at 84×.

of these lateral connections. Higher draw ratios would therefore not necessarily increase further the tendency for fibrillation.

Since the polymer's strong covalent bonds are increasingly aligned in the load-bearing direction by the molecular orientation imparted by the drawing process, it is natural to expect a correlation between strength and orientation. Such a correlation was established definitively in the case of polypropylene in a classic structure–property study by researchers at Hercules, Inc. and the University of Delaware in the 1960's and 70's. This study is summarized in a monograph by Samuels.[11]

Figure 15 is reproduced from the Samuels monograph, showing how the strength of drawn polypropylene correlates with the orientation induced by processing. The change is slope exhibited by the Samuels data at $f \approx 0.7$ marks the spherulite-to-axial transformation. The orientation and strength of the Cu-7 tail string is plotted on this

same graph, showing that its ratio of strength to orientation is typical of polypropylene. The graph shows that the Cu-7 string has been drawn to moderate levels, into the fibrillar region but far from what could be termed "ultraoriented." Bigg[19] cites studies in which polypropylene has been drawn to a stretch ratio of 27 to 1, producing a modulus of 7.3 Mpsi, as opposed to the ≈ 1 Mpsi measured for the polypropylene tail string (see Fig. 4). The draw ratio employed in the Cu-7 tail string does not appear to be excessive: it is midrange for polypropylene as shown in Figure 15, and the resulting molecular orientation is comparable to the ParaGard string. The tendency for occasional fibrillation is a natural consequence of molecular alignment.

Orientation processing of polymers does tend to produce a small amount of interval voiding in the material, more if particulate fillers are present to generate the "breakout" phenomenon described earlier. However, there
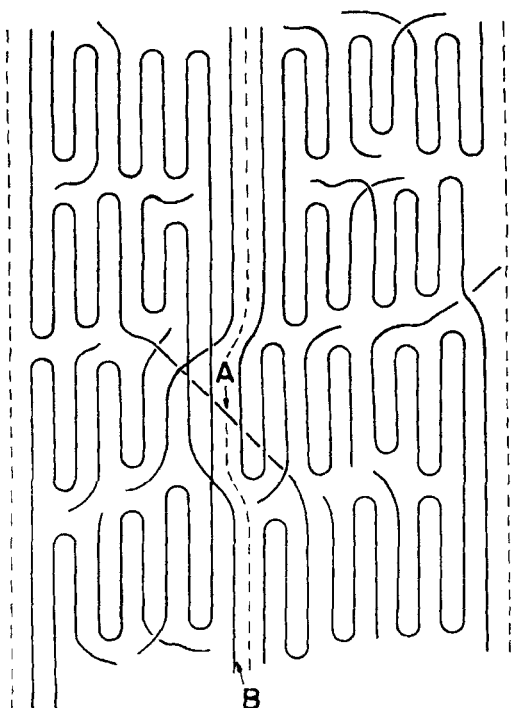
Figure 14. Schematic illustration of fibrillar microstructure of drawn polymer fibers.

Among their principal advantages, the olefinic fibers are biologically inert and well established for use in biological environments,[20] they resist moisture uptake or transport due to their natural hydrophobicity, and they can be processed by drawing to achieve the strength needed in this application. Although increasing the strength of a polymer in one direction unavoidably increases the tendency for fibrillation, it does not appear that fibrillation is sufficient to produce deleterious consequences in IUD tail strings. Polypropylene processed to have sufficient tensile strength for an IUD tail string may exhibit an increased tendency to fibrillate during handling compared to polyethylene. However, its capacity to accept attachment by heat bonding yields a tail string composed of a single strand of thin flexible monofilament.

is no evidence that whatever voids are present in either of the two strings studied here have degraded the mechanical properties or the resistance of the material to environmental agents such as wetting or nonwetting liquids. The load-bearing molecular paths flow around the elongated voids rather than being interrupted by them, and the strengths of the polypropylene strings are in close agreement with those expected based on their measured molecular orientations.

In summary, both polyethylene and polypropylene are appropriate choices for tail string materials when viewed against the list of criteria proposed earlier.
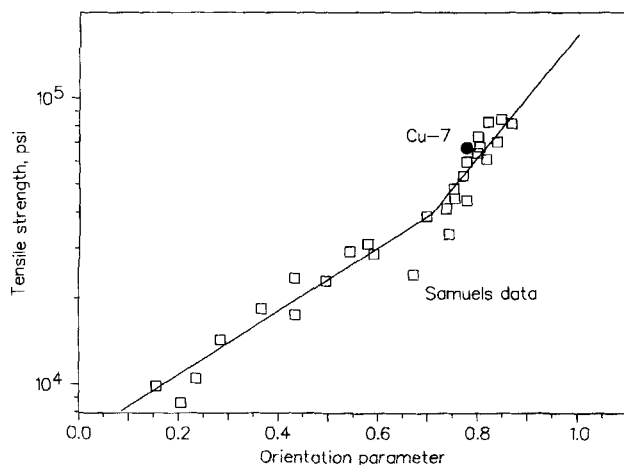

Figure 15. Correlation between drawn-induced molecular orientation and resulting fiber strength for polypropylene.

REFERENCES

1. Intra-Uterine Devices: Physiological and Clinical Aspects, World Health Organization Technical Report Series, Vol. 397, 1968.
2. Warner, M. S.; Matsuno, S. J.; Virgin, C. J.; et al. Performance of the polypropylene fiber tailstring on the copper 7 intrauterine device, J. Appl. Biomater. 2:73–94; 1991
3. Cu-7 New Drug Application 17-408, 1st Semiannual Surveillance Report, September 17, 1975.
4. Costerton, J. W.; Geesey, G. C.; Cheng, K.-J. How Bacteria Stick. Sci. Am. 238:86–95; 1978.
5. Ahmed, M. Polypropylene fibers—Science and technology. New York: Elsevier; 1982.
6. The value of 170 J/g is recommended by Himont Inc. as the crystalline heat of fusion for their ProFax resins.
7. Brandrup, J.; Immergut, E. H. Editors. Polymer handbook. 2nd ed., Chap. V, New York: John Wiley & Sons; 1975:14–16.
8. Armond, V. J.; Atkinson, J. R. Chromic acid as an etchant for bulk polypropylene and its use to study (i) nitric acid attack on polypropylene (ii) cracks in polypropylene induced by tensile stress. J. Mater. Sci. 4:509–517; 1969.
9. Miller, B. The wetting of fibers, In: Schick, M. J., Ed. Surface characteristics of Fibers and Textiles, New York: Marcel Dekker; 1977.
10. Moseley, W. W. The measurement of molecular orientation in fibers by acoustic methods. J. Appl. Polym. Sci. 3:266–276; 1960.
11. Samuels, R. J. Structured polymer properties. New York: John Wiley & Sons, 1974.
12. Baccaredda, M.; Butta, E. Proprietà meccaniche dinamiche e transizioni isofasiche nei Polietileni lineari e in alcune poli-alfa-olefine. La Chimica e L'Industria, (Milan) 44:1228–1236; 1962.
13. Morgan, H. Correlation of molecular orientation in fibers by optical birefringence and pulse velocity. Textile Res. J. 32:866–868; 1962.

14. Alexander, L. E. X-Ray diffraction methods in polymer science. New York: John Wiley & Sons; 1969.

15. Wilchinsky, Z. W. Measurement of orientation in polypropylene film. J. Appl. Phys. 31:1969–1972; 1960.

16. Richardson, T. L. Industrial plastics: theory and application. Albany, NY: Delmar Publishers, Inc.; 1989.

17. Peterlin, A. Molecular model of drawing polyethylene and polypropylene. J. Mater. Sci. 6:490–508; 1971.

18. Peterlin, A. Morphology and properties of crystalline polymers with fiber structure. Textile Res. J. 42(1):20–30; 1972.

19. Bigg, D. M. Mechanical property enhancement of semicrystalline polymers—A review. Polym. Eng. Sci. 28:830–841; 1988.

20. Halpern, B. D.; Tong, Y.-C. Medical applications. In: Encyclopedia Polymer Science and Engineering, New York: Wiley; 1986.